NASA TT F-65

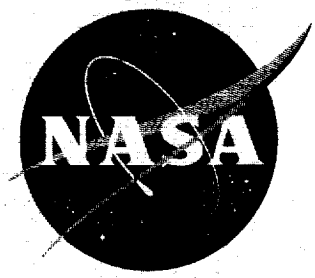

TECHNICAL TRANSLATION

F-65

MODEL EXPERIMENTS ON ATOMIZATION OF LIQUIDS

By Mintscho Popov

Translation of "Modellversuche mit Flüssigkeitszerstäubung." Acad. Rep. Populare Române, Rev. de Mécanique Appliquée (Bucharest), t. 1, no. 1, 1956, pp. 71-88.

NATIONAL AERONAUTICS AND SPACE ADMINISTRATION

WASHINGTON July 1961

NATIONAL AERONAUTICS AND SPACE ADMINISTRATION

TECHNICAL TRANSLATION F-65

MODEL EXPERIMENTS ON ATOMIZATION OF LIQUIDS*

By Mintscho Popov

ABSTRACT

The purpose of this paper is to determine the similarity laws for the atomization of liquids with constant material properties and to verify them by comparison model experiments.

The analyses show that the effect of the viscosity of the gas was very small and that approximate model experiments can be carried out without considering the ratio M of the gas to liquid viscosity, a condition that is difficult to satisfy.

The derived and experimentally verified similarity laws permit the modeling of the atomization processes of liquids whereby considerable simplifications in experimental procedure and generalization of the experimental data are made possible.

I. OBJECT OF STUDY

The laws for the complex atomization of liquids have not as yet been obtained analytically owing to the great mathematical difficulties encountered. The investigation of atomization is therefore being conducted mainly through experiment. This method is also associated with great difficulties that are largely due to the small size and the relatively large velocities of the droplets formed. The introduction of model tests can considerably facilitate the investigation by making larger dimensions and smaller velocities possible; furthermore, the similarity permits a generalization of the experimental results to dynamically similar systems.

The object of the present study is to determine the similarity laws for the atomization of liquids for the more simple case of constant physical properties of the material and to verify them by comparative model experiments.

*"Modellversuche mit Flüssigkeitszerstäubung." Acad. Rep. Populare Románe, Rev. de Mécanique Appliquée (Bucharest), t. 1, no. 1, 1956, pp. 71-88.

II. MECHANISM OF ATOMIZATION PROCESS OF LIQUIDS

In order to derive the similarity laws a knowledge of the physical process (as accurate as possible) is required. The atomization process is briefly described in the following section.

The atomization of liquids in technical apparatus is generally effected by having the liquid to be atomized flow out of the orifice of a nozzle into a gas medium where it disintegrates into noncohering particles that pass over into droplets.

Two fundamental types of atomization are distinguished as follows: (a) Hydraulic atomization, in which the gas medium is practically at rest while the liquid issues with large velocity and supplies the energy required for the atomization, and (b) Pneumatic atomization in which the gas velocity is considerably greater than that of the liquid and the gas stream provides the atomization energy.

We shall here consider mainly hydraulic atomization although pneumatic atomization will also be taken into account in deriving the model laws.

Depending on the exit velocity of the liquid the breaking up takes place in several typical forms.

At very small exit velocities (quasistatic case), the droplet formation at the nozzle mouth takes place as shown in figure 1, which presents a sequence of moving picture photographs for a vertical nozzle. The weight of the suspended drop is balanced by the surface tension. When, with a further supply of liquid, the drop has reached a limiting size it breaks off under the action of gravity and tends towards the stable spherical form.

At sufficiently small velocities this process called dripping occurs, as Lohnstein (ref. 1) has shown, under the action of gravity and surface tension, that exerts a force σ kg/m per unit length tangential to the surface.

Through the action of the surface tension between the liquid and the adjoining gas a pressure difference arises according to the Laplace equation

$$p = p_g + \sigma\left(\frac{1}{R_1} + \frac{1}{R_2}\right), \tag{1}$$

where p is the liquid pressure, p_g the gas pressure, and R_1 and R_2 are the principal radii of curvature of the surface element under consideration (in the following paragraphs the magnitudes referring to the gas medium are denoted by the subscript g).

At larger exit velocity of the liquid the drop formation at the nozzle mouth ceases and the liquid then issues in the form of a cylindrical jet. However, under the action of the surface tension the cylindrical jet is unstable; the irregularities due to initial disturbances at its surface are increased by the surface tension. The jet narrows down at several places and at a certain distance from the mouth (the break-down distance) it disintegrates into noncohering particles, that later draw together into spheres, as shown by the investigations of Haenlein (ref. 2) and Weber (ref. 3). Figure 2 shows a sequence of motion pictures of the disintegration of such a liquid jet into drops. (Figs. 1 and 2 are taken from work by Ohnesorge (ref. 8).)

The drop formation takes place mainly under the action of the surface tension while the effect of the gravity force becomes increasingly smaller with increasing velocity. Here, however, the viscosity forces of the liquid also enter as a resistance to the disintegration.

At still greater exit velocities of the liquid the inertia forces come into play. These forces are proportional to the square of the velocity, give rise to pressure differences, and under certain conditions may constitute the principal cause for the jet disintegration. This condition occurs if the liquid stream has already become turbulent within the nozzle. The liquid particles (also termed liquid globules) then have transverse motions in various directions. On leaving the nozzle, freed from the boundaries of the wall, the liquid particles separate from one another. The jet breaks down into noncohering parts, predominantly in the form of filaments and films, from which spherical drops are then formed.

Figure 3 shows a sequence of high-speed photographs (25,000 pictures per sec[1]) of the disintegration of a methanol jet with an exit velocity of 52 meters into a vacuum (about 100 mm Hg), that was applied to eliminate the effect of the gas forces to a large extent. Both the shape of the disintegrated particles and the widening of the jet transverse to the stream direction may be seen due to the turbulent transverse motions of the liquid particles. The disintegration process is favored by the intensity of the turbulence, which in turn results from the initial disturbances (formation of vortices by sharp edges, curvatures, etc.) in the nozzle orifice.

Here considerably smaller drops are formed as compared with the drop formation according to figure 2. Owing to the larger velocities

---

[1]A description of the apparatus used is given in "Investigation of the Atomization of a Jet from an Injection Nozzle with Varying Expansion Angle," by Mintscho Popov. Annuaire de l'Ecole polytechnique d'Etat "Stalin," Sofia, 1953/1954.

the effect of the viscosity forces is correspondingly greater; the gravity forces, however, no longer have any effect on the jet disintegration and drop formation.

In the analytical treatment of the liquid stream for constant coefficients of the material and considering all the participating forces we must begin with the Navier-Stokes differertial equation

$$\frac{\partial \vec{v}}{\partial t} + (\vec{v}\ \text{grad})\ \vec{v} = \vec{g} - \frac{1}{\rho}\ \text{grad}\ p + \frac{\mu}{\rho}\ \Delta\vec{v} \qquad (2)$$

and the continuity equation

$$\text{div}\ \vec{v} = 0 \qquad (3)$$

where t denotes the time, g the earth's acceleration, v the velocity, ρ the mass density, p the pressure and μ the liquid viscosity.

For large relative velocities between the liquid jet and the surrounding gas, the gas forces are also appreciable, exerting normal pressures and tangential stresses on the liquid surface. As already shown by the investigations of Haenlein (ref. 2) and Weber (ref. 3) mentioned previously, the normal pressures enlarge the initial unevennesses on the jet surface, reduce the breakdown length and thereby favor the jet disintegration.

Figures 4 and 5 show the jet disintegration for higher air pressure but otherwise same test conditions as in figure 3; figure 4 corresponds to atmospheric pressure and figure 5 to an excess pressure of 2 atmospheres. Comparison with figure 3 shows that the gas forces increasing with the gas density considerably influence the jet decomposition by shortening the breakdown distance, increasing the jet expansion and producing the formation of smaller particles or drops.

A very considerable effect of the gas forces is that under given conditions they may further subdivide the particles already formed in the jet disintegration into drops of very small dimensions. The process for free water drops in an airstream was investigated and was named "blowing apart" by Hochschwender (ref. 4).

Figure 6 shows high velocity moving picture photographs (25,000 pictures per sec) of a "blowing apart" process. The liquid jet has small initial disturbances and therefore maintains its cylindrical form at relatively large distances. Due to fluctuations of the exit velocities and eddies nodular thickenings are formed at several points over its length that are particularly exposed to the action of the air. While the front surface is acted upon by excess air pressure, below atmospheric pressures arise at the periphery. These pressures draw the thickenings

outward in the radial direction until they go over into thin conical films that finally burst into many very small drops (not individually recognizable in the pictures). A similar blowing apart occurs in the case of many particles formed during jet disintegration and results in the final formation of extremely small droplets.

From the discussion on the effect of the gas forces it is concluded that larger relative velocities between liquid and gas, that as a rule are applied in technical installations, can considerably affect the jet disintegration, the blowing apart and therefore the atomization as a whole.

In the analytical treatment of the gas flow it is similarly necessary to begin with the Navier-Stokes differential equation

$$\frac{\partial \vec{v}_g}{\partial t} + (\vec{v}_g \text{ grad}) \vec{v}_g = \vec{g} - \frac{1}{\rho_g} \text{grad } p_g + \frac{\mu_g}{\rho_g} \Delta \vec{v}_g \tag{4}$$

and the continuity equation

$$\text{div } \vec{v}_g = 0 \tag{5}$$

Here too constant material properties are assumed.

The mathematical solution of the problem requires the integration of the system consisting of equations (2), (3), (4) and (5), wherein a series of initial and boundary conditions must be satisfied.

One boundary condition is represented by the Laplace equation (1), that must be satisfied for each point of the liquid surface and hence also for the final spherical drop with the diameter d. Owing to $R_1 = R_2 = d/2$ equation (1) can be written in the form

$$p = p_g + \frac{4\sigma}{d} \tag{6}$$

Further boundary conditions are given by the distributions of the liquid velocity v_{gr} and of the gas velocity $v_{g,gr}$ at the exit orifices to the system; they may be given by the following functions:

$$\vec{v}_{gr} = \vec{\varphi}(\vec{r}, \nu, t) \tag{7}$$

and

$$\vec{v}_{g,gr} = \vec{\varphi}_g(\vec{r}_g, \nu_g, t), \tag{8}$$

where $\vec{r}$ and $\vec{r}_g$ are radii vectors that describe the outlet cross sections. The functions φ and φ_g also involve the kinematic viscosities ν and ν_g because, from dimensional considerations for steady flows, the velocities cannot be functions of only one radius vector (length).

Boundary conditions that cannot be influenced by external effects are the equality of the velocities and of the tangential stresses at the boundary between liquid and gas. In addition the relative velocity between the liquid or gas and the fixed walls must be equal to zero.

As stated previously, the obtained system of equations cannot be solved mathematically for the general case of liquid atomization. Considering the boundary conditions, however, the system can be employed for finding the similarity or model laws.

III. MODEL LAWS

A knowledge of the similarity theory, discussed by Kirpitschev (ref. 5), Eigenson (ref. 6), Weber (ref. 7) and others, is here assumed. From this theory it is known that the full-scale processes (that occur in practice) and the model processes (used in the investigation) are similar if the two systems are geometrically similar, there is equality of the dimensionless criteria, and the equal dimensionless boundary and initial conditions are given.

The similarity criteria are found from the equations that describe the process and its boundary conditions, by transforming them into dimensionless form. The boundary conditions, that cannot be affected by external actions, need not be considered since they are automatically satisfied by the natural laws.

For the atomization for the case of constant material properties equations (2), (3), (4), (5), (6), (7) and (8) must be reduced to dimensionless form. For this purpose the following relative units of measure are introduced: l_o diameter of the exit orifice for the liquid, t_o duration of the process or a definite phase of the process, $v_m = 4Q/\pi l_o^2 t_o$ mean exit velocity of the liquid, computed from the outflowing volume Q during the time t_o, p_o pressure at a definite point of the system, g acceleration of gravity, ρ, μ, and σ the constants density, viscosity and surface tension of the liquid, respectively. We can then write

$$\vec{v} = v_m\vec{V},\ \vec{v}_g = v_m\vec{V}_g,\ \vec{v}_{gr} = v_m\vec{V}_{gr},\ \vec{v}_{g,gr} = v_m\vec{V}_{g,gr},\ x = l_oX,\ y = l_oY,$$

$$z = l_oZ,\ \vec{l} = x\vec{i} + y\vec{j} + z\vec{k} = l_o\vec{L} = l_o(X\vec{i} + Y\vec{j} + Z\vec{k}),\ \vec{r} = l_o\vec{R},\ \vec{r}_g = l_o\vec{R}_g,$$

$$d = l_oD,\ p = p_oP,\ t = t_oT,\ \mu_g = \mu M,\ \rho_g = \rho N,$$

where the capital letters denote the corresponding dimensionless magnitudes; for example, $\vec{V}$, $\vec{V}_g$, $\vec{V}_{gr}$, and $\vec{V}_{g,gr}$ denote the dimensionless velocities, X, Y, Z denote the dimensionless coordinates, and so forth.

If we take into account that the scalar components of $\partial\vec{v}/\partial t$ are of the form $\partial v_x/\partial t$, those of $\vec{v}$ grad $\vec{v}$ of the form $\partial v_x^2/\partial x$, those of grad p of the form $\partial p/\partial x$, those of $\Delta\vec{v}$ of the form $\partial^2 v_x/\partial x^2$ and those of div $\vec{v}$ of the form $\partial v_x/\partial x$, then equations (2) to (8) can be transformed as follows

$$\frac{v_m}{t_o}\frac{\partial\vec{V}}{\partial T} + \frac{v_m^2}{l_o}(\vec{V}\ \text{grad})\vec{V} = \vec{g} - \frac{1}{\rho}\frac{p_o}{l_o}\ \text{grad}\ P + \frac{\mu}{\rho}\frac{v_m}{l_o^2}\Delta\vec{V}, \tag{9}$$

$$\frac{v_m}{l_o}\ \text{div}\ \vec{V} = 0, \tag{10}$$

$$\frac{v_m}{t_o}\frac{\partial\vec{V}_g}{\partial T} + \frac{v_m^2}{l_o}(\vec{V}_g\ \text{grad})\vec{V}_g = \vec{g} - \frac{1}{\rho N}\frac{p_o}{l_o}\ \text{grad}\ P_g + \frac{\mu}{\rho}\frac{M}{N}\frac{v_m}{l_o^2}\Delta\vec{V}_g, \tag{11}$$

$$\frac{v_m}{l_o}\ \text{div}\ \vec{V}_g = 0, \tag{12}$$

$$p_o P = p_o P_g + \frac{\sigma}{l_o}\frac{4}{D}. \tag{13}$$

In order to reduce these equations to dimensionless form, equations (9) and (11) are divided by v_m^2/l_o and equation (13) is divided by p_o while in the case of equations (10) and (12), it is taken into account that $v_m/l_o \neq 0$. The following dimensionless equations are obtained:

$$\frac{l_o}{v_m t_o}\frac{\partial\vec{V}}{\partial T} + (\vec{V}\ \text{grad})\vec{V} = \frac{\vec{g}l_o}{v_m^2} - \frac{p_o}{\rho v_m^2}\ \text{grad}\ P + \frac{\mu}{\rho v_m l_o}\Delta\vec{V}, \tag{14}$$

$$\text{div}\ \vec{V} = 0, \tag{15}$$

$$\frac{l_o}{v_m t_o}\frac{\partial\vec{V}_g}{\partial T} + (\vec{V}_g\ \text{grad})\vec{V}_g = \frac{\vec{g}l_o}{v_m^2} - \frac{p_o}{\rho v_m^2}\frac{1}{N}\ \text{grad}\ P_g + \frac{\mu}{\rho v_m l_o}\frac{M}{N}\Delta\vec{V}_g, \tag{16}$$

$$\text{div}\ \vec{V}_g = 0, \tag{17}$$

$$P = P_g + \frac{\sigma}{p_o l_o}\frac{4}{D}. \tag{18}$$

After introducing the respective measuring units l_o, v_m, μ, ρ, and t_o into equations (7) and (8) there are obtained

$$v_m\vec{V}_{gr} = \vec{\varphi}(l_o\vec{R},\ \nu,\ t_oT) \tag{19}$$

and

$$v_m\vec{V}_{g,gr} = \vec{\varphi}_g\left(l_o\vec{R}_g,\ \nu\frac{M}{N},\ t_oT\right). \tag{20}$$

The preceding procedure applied for reducing the equations to dimensionless form cannot further be used here since equations (19) and (20) are not given in concrete form. We can nevertheless in this case use the fact that the terms of the functions φ and φ_g must have the dimension of a velocity. Since their arguments $\vec{R}$, $\vec{R}_g$ and T are dimensionless the coefficients, which evidently are made up of the magnitudes l_o, ν, and t_o, must have this dimension (m/s). However, only two combinations of this kind

$$l_o/t_o \quad \text{and} \quad \nu/l_o,$$

need to be taken into account; all the remaining combinations of powers of l_o, ν, and t_o that have the dimension m/s may, as is easy to prove[2], be formed by the power products of these two combinations. The coefficients of the functions φ and φ_g can naturally also be composed of the sums of such combinations.

If equations (19) and (20) are divided by v_m, there are obtained on the left side the dimensionless velocities $\vec{V}_{gr}$ and $\vec{V}_{g,gr}$ and on the right side from l_o/t_o and ν/l_o, the dimensionless criteria

$$\frac{l_o}{t_o v_m} = Ho^{-1} \quad \text{and} \quad \frac{\nu}{v_m l_o} = Re^{-1}$$

---

[2]The most general combination of l_o, ν, and t_o has the form $l_o^k\nu^p t_o^q$ and is subject to the condition

$$\left[l_o^k\nu^p t_o^q\right] = ms^{-1} \quad \text{or} \quad m^k m^{2p} s^{-p-q} = ms^{-1}.$$

By comparison of the dimensions there is obtained

$$k + 2p = 1 \quad \text{and} \quad q - p = -1.$$

From this follows $k = 1 - 2p$, $q = p - 1$ and $l_o^k\nu^p t_o^q = (l_o/t_o)^{1-p}(\nu/l_o)^p$, where p may be arbitrary, as was to be proved.

where Ho is the so-called criterion for homochronism and Re is the Reynolds number.

From the preceding considerations it is seen that all the remaining coefficients of equations (19) and (20) give criteria that are made up of Ho and Re. Equations (19) and (20) can therefore be reduced to the following dimensionless form

$$\vec{V}_{gr} = \vec{\Phi}(\mathrm{Re},\ \mathrm{Ho},\ \vec{R},\ T), \tag{21}$$

$$\vec{V}_{g,gr} = \vec{\Phi}_g(\mathrm{Re},\ \mathrm{Ho},\ M,\ N,\ \vec{R}_g,\ T). \tag{22}$$

The integration of the system of differential equations (14) to (17) with account taken of boundary conditions (18), (21) and (22), would give the functions for $\vec{V}$, $\vec{V}_g$, P, P_g and D, that will evidently contain the place vector $\vec{L}$, the time T, the velocities $\vec{V}_{gr}$ and $\vec{V}_{g,gr}$ and the coefficients occurring in the dimensionless equations.

For practical purposes the size of the formed drops is of most interest. In the following paragraphs, therefore, only the function for $D = d/l_o$ is discussed, which is of the form

$$D = \psi\left(\frac{l_o}{v_m t_o},\ \frac{\vec{g} l_o}{v_m^2},\ \frac{p_o}{\rho v_m^2},\ \frac{\mu}{\rho v_m l_o},\ \frac{\sigma}{p_o l_o},\ M,\ N,\ \vec{V}_{gr},\ \vec{V}_{g,gr},\ \vec{L},\ T\right) \tag{23}$$

All the expressions appearing in the equations are dimensionless and represent the similarity criteria; the first five on the right side of the equation are "criteria complexes" and the remaining are "criteria simplexes." Equation (23) is the so-called criterial equation and is to be determined by experiment.

It is known that every similarity criterion can be replaced by the exponential product formed with any other criteria of the criterial equation. We may for example substitute for $\sigma/p_o l_o$

$$\left(\frac{\sigma}{p_o l_o}\right)^{-1/2}\left(\frac{p_o}{\rho v_m^2}\right)^{-1/2}\frac{\mu}{\rho v_m l_o} = \frac{\mu}{\sqrt{\sigma\rho l_o}} = Z,$$

that represents the criterion, introduced by Ohnesorge (ref. 8), for the jet disintegration without the effect of the gas forces.

Furthermore, in equation (23) $l_o/v_m t_o = \mathrm{Ho}^{-1}$, $\vec{g} l_o/v_m^2 = \mathrm{Fr}^{-1}$, where Fr denotes the Froude criterion, $p_o/\rho v_m^2 = \mathrm{Eu}$ the Euler criterion, and

$\mu/\rho v_m l_o = \nu/v_m l_o = Re^{-1}$. Equation (23) can therefore be reduced to the following form

$$D = \psi\left(\frac{v_m t_o}{l_o}, \frac{v_m^2}{\vec{g} l_o}, \frac{p_o}{\rho v_m^2}, \frac{v_m l_o}{\nu}, \frac{\mu}{\sqrt{\sigma \rho l_o}}, M, N, \vec{V}_{gr}, \vec{V}_{g,gr}, \vec{L}, T\right)$$

$$= \psi(Ho, Fr, Eu, Re, Z, M, N, \vec{V}_{gr}, \vec{V}_{g,gr}, \vec{L}, T). \qquad (24)$$

For similar processes there must be equality of the corresponding criteria. For example, it is required that for the full scale (magnitudes denoted by "prime") and for the model (magnitudes denoted by "double prime") there is equality of the first complex Ho:

$$\frac{v_m' t_o'}{l_o'} = \frac{v_m'' t_o''}{l_o''}.$$

Owing to $v_m = 4Q/\pi l_o^2 t_o$ the equation goes over into the form

$$\frac{Q'}{l_o'^3} = \frac{Q''}{l_o''^3}, \text{ or } \frac{Q'}{Q''} = \frac{l_o'^3}{l_o''^3}$$

and states that the outflowing liquid volume Q' of the full scale and of the model Q'' must, during the corresponding times t_o' and t_o'', stand in the same ratio as the volumes $l_o'^3$ and $l_o''^3$ or the volumes of the systems. However this geometric condition is evidently satisfied by the function of the limiting velocities according to equation (21); hence the criterion Ho need not be further considered.

With the assumption made of constant material properties, among them ρ_g = constant, the Euler criterion Eu may, as is known, drop out of the criterial equation.

As was shown in the discussion on the atomization mechanism, at large velocities there is practically no effect of the gravitational forces on the drop formation. The Froude criterion Fr, that takes into account the effect of gravitational forces, may therefore similarly be omitted.

The criterial equation (24) for the liquid atomization at large velocities and constant material properties can therefore be reduced to the following simplified form:

$$D = \psi(Re, Z, M, N, \vec{V}_{gr}, \vec{V}_{g,gr}, \vec{L}, T) \qquad (25)$$

From the similarity conditions Re' = Re" and Z' = Z", and from the fundamental dynamical equation (force = mass × acceleration) the transfer ratios are determined as follows:

$$\text{for all corresponding lengths} \quad C_l = \frac{l'}{l''} = \frac{\mu'^2\sigma''\rho''}{\mu''^2\sigma'\rho'}, \tag{26}$$

$$\text{for all corresponding times} \quad C_t = \frac{t'}{t''} = \frac{\mu'^3\sigma''^2\rho''}{\mu''^3\sigma'^2\rho'}, \tag{27}$$

$$\text{for all corresponding forces} \quad C_k = \frac{K'}{K''} = \frac{\mu'^2\rho''}{\mu''^2\rho'}. \tag{28}$$

From these equations the transfer ratios for all remaining mechanical magnitudes can be computed; for the velocities there is obtained

$$C_v = \frac{v'}{v''} = \frac{C_l}{C_t} = \frac{\mu''\sigma'}{\mu'\sigma''}. \tag{29}$$

It is seen that the transfer ratios cannot be arbitrarily chosen because they depend on the material constants of the model liquid. It also follows that simultaneous increase of the dimensions $C_l < 1$ and decrease of the velocities $C_v > 1$ can be attained in the model by choosing for the model a liquid with greater viscosity $\mu'' > \mu'$ smaller surface tension $\sigma'' < \sigma'$ and smaller mass density $\rho'' < \rho'$.

The criteria $M = \mu_g/\mu$ and $N = \rho_g/\rho$ are satisfied by using in the model a gas whose viscosity and mass density are in the same ratio to those of the model liquid as in the full scale.

The most difficult to satisfy are the time and space varying criteria $\vec{V}_{gr}$ and $\vec{V}_{g,gr}$, since the experimental determination of their functions, equations (21) and (22), is connected with great difficulties. These difficulties can be circumvented by also including the atomization nozzle, the pipes and the pumps (for liquid and gas) in the experimental system and designing them in a similar manner. The elements (sharp edges, curvatures, etc.) producing the initial disturbances should be made geometrically similar with particular care, since the turbulence mostly depends on these elements. Similarly the elastic pressure fluctuations in the pump-pipe-nozzle system, that can also be modeled according to the modeling laws derived by Lindner (ref. 9), are to be considered.

In nonsteady atomization processes account must also be taken of the initial conditions in each case. In the most general case these conditions are satisfied by having equal space distribution of both the dimensionless liquid and gas velocities in the system at the start of

the process, $T = 0$. It is advantageous to begin counting the time at the start of the liquid stream, so that for $T = 0$, also $\vec{V} = 0$. However, if a gas flow exists at this instant of time, $\vec{V}_g \neq 0$, the spatial distribution of its dimensionless velocity must be taken into account. In the simplest case there are no liquid and gas flows at the start of the atomization process.

For satisfied similarity conditions drops with equal dimensionless diameters $D' = D''$ will be obtained at corresponding times $T' = T''$ and corresponding points $\vec{L}' = \vec{L}''$. For the complete estimate of the fineness of the atomization all drops that occur at corresponding times in corresponding regions should be measured and from these measurements the mean drop diameter and frequency distribution can be determined, which for similar processes must give equal numerical values in relative measuring units.

IV. MODEL TESTS

In order to test the derived similarity laws comparison model tests with hydraulic atomization were conducted. The atomization took place in a closed chamber without any specific air motion so that the ratio $\vec{V}_{g,gr}$ did not have to be considered. Furthermore, a quasistationary (stationary in the time mean value) flow was set up so that the comparisons of the results could be carried out in statistical mean values without taking account of the dimensionless time T and the initial conditions.

The full scale atomization nozzle had an exit opening with the diameter $l'_o = 1$ mm and served for the atomization of water with material constants $\rho' = 102$ kg s^2/m^4, $\mu' = 1.08 \times 10^{-4}$ kg s/m^2 and $\sigma' = 74.3 \times 10^{-4}$ kg/m in air with $\rho'_g = 0.122$ kg s^2/m^4 and $\mu'_g = 1.83 \times 10^{-6}$ kg s/m^2.

Both media had the same temperature (20° C) and the velocities were small compared with the velocity of sound so that the condition of constant material properties was well satisfied.

As model liquid, carbon tetrachloride (CCl_4) was used with the material constants $\rho'' = 162$ kg s^2/m^4, $\mu'' = 1.02 \times 10^{-4}$ kg s/m^2 and $\sigma'' = 26.1 \times 10^{-4}$ kg/m.

From equations (26) and (29) the following transfer ratios are computed:

$$\text{for the lengths } C_l = l'/l'' = 1/1.6$$

$$\text{and for the velocities } C_v = v'/v'' = 2.68.$$

With this model liquid, therefore, a 1.6 times linear magnification of the model and a 2.68 times reduction of the velocities and equality of the criteria Re and Z from equation (25) for the full scale and for the model can be attained. There is further determined

$$Z' = Z'' = Z = 0.39 \times 10^{-2}$$

The ratio M for the full scale is computed as

$$M' = \frac{\mu_g'}{\mu'} = 1.7 \times 10^{-2}$$

Because of the small difference of the viscosities of water and carbon tetrachloride (only about 6 percent) air can also be used as the gas for the model and sufficient agreement of M' and M'' is attained.

For the full scale the ratio N is computed as

$$N' = \frac{\rho_g'}{\rho'} = 1.2 \times 10^{-3}$$

In order to obtain the same numerical value for the model the mass density of the air must be increased to

$$\rho_g'' = \rho'' \times 1.2 \times 10^{-3} = 0.194 \text{ kg s}^2/\text{m}^4$$

which can be done through suitable increase of the air pressure in the test chamber. It is noted here that the increase of the air density (from 0.122 to 0.194) has practically no effect on the values of μ'' and σ'' measured at atmospheric pressure.

The boundary condition $\vec{V}_{gr}' = \vec{V}_{gr}''$ was satisfied by having accurate geometrical similarity of the nozzles and their supply pipes while the outflows of the liquids were produced by suitable constant pressures in the liquid container.

The investigation of the atomizations was conducted by photography using electric spark illumination of very short duration (about 10^{-6} sec) which enabled sharp pictures to be obtained even at large velocities of the atomization jets.

Figure 7 shows the similarly set up atomizating jets of the full scale (above) for medium exit velocity $v_m' = 44.2$ m/s and of the model (below) for $v_m'' = 16.5$ m/s and for Re' = Re'' = Re = 41,800. The full scale picture is linearly magnified 1.6 times so that the two jets appear

to be of equal dimensions, a circumstance which facilitates their comparison. On account of the great experimental difficulties the pictures were not taken at corresponding times $T' = T''$ so that due to the turbulence there is no complete geometric similarity; nevertheless, a certain similarity will be recognized.

Figure 8 shows the similar jets at larger velocities $v_m' = 62.6$ m/s and $v_m'' = 23.3$ m/s and $Re' = Re'' = Re = 59,100$.

In order to enable quantitative comparison of the similar atomizations, pictures of the atomizing jet were taken in similarly situated regions of the system (at the distance of about 130 l_o from the nozzle orifice) where the atomizations were completed, all the drops were measured under the microscope, were counted according to their magnitude, and their frequency (disperse distribution) determined.

Figures 9 and 10 show the results for Re = 41,800 and Re = 59,100; the dimensionless drop diameter $D = d/l_o$ is laid off on the abscissa axis and the frequency in percent plotted as ordinate. Both figures show that the points of full scale and model show good agreement in the frequency curves.

Figure 11 shows the dimensionless mean drop diameter $D_m = d_m/l_o$ determined from the measured drops for full scale and model plotted as a function of the Reynolds number Re. Here too the points corresponding to full scale and model fall quite satisfactorily on a common curve.

The results presented in the preceding figures show convincingly that the satisfying of the criteria of equation (25) does in fact result in similarity of the atomizations.

V. EFFECT OF THE GAS VISCOSITY

As was previously stated, in order to obtain enlargement of the dimensions and reduction of the velocities in the model it is necessary to choose a model liquid with larger viscosity and smaller surface tension and mass density. The liquids used in practice for atomizations generally, however, have small surface tensions and mass densities. It is therefore almost impossible to discover a model liquid with such small surface tensions and mass densities so as to give an essential enlargement of the model; this can be attained principally through the choice of a model liquid with greater viscosity. It follows, however, from the similarity condition $M' = M''$, or $\mu_g'/\mu' = \mu_g''/\mu''$, that the viscosity of the model gas must be increased in the same ratio as that of the model liquid. For equal temperature, however, the viscosities of the gases do not differ very much from each other; neon, for example, has the greatest

viscosity and is only 1.7 times as large as that of the air. This circumstance imposes limitations on the model enlargement.

Therefore the question arises as to the extent to which the similarity is disturbed if the criterion M is not satisfied and a gas with smaller viscosity is employed in the model. The answer is to be sought in the effect of the gas forces on the atomization process.

As already stated, the gas exerts on the liquid surface normal and tangential stresses which affect the disintegration and blowing apart of the jet. Under otherwise equal conditions the normal pressures are proportional to the mass density while the tangential stresses are proportional to the viscosity. Consequently the change of the gas viscosity will above all affect the tangential stresses.

It is known that the ratio of the forces exerted on bodies in a fluid stream which sometimes result from the normal pressures and sometimes result from the tangential stresses (corresponding to the so-called pressure and friction resistances) depends on the Reynolds number and on the shape and position of the bodies.

The Reynolds number, computed from the dimension of the body and the relative velocity, is a measure of the ratio of the pressure to the tangential forces. Hence the effect of the tangential forces decreases with increasing Reynolds number.

Figures 7 and 8 show that the liquid particles formed during the jet disintegration have dimensions that are larger in part than the nozzle diameter. To a first approximation their dimensions can be set equal to the nozzle diameter l_o and their relative velocity to the air set equal to the exit velocity v_m. The order of magnitude of the Reynolds number of the airflow for the atomization in figure 7 is then found to be about 2800 and for the atomization in figure 8 about 4000. As is known from the resistance theory, for such Reynolds numbers and for bodies, such as spheres, cylinders and plates, in transverse flow the friction forces are very small as compared with the pressure forces.

Figures 7 and 8 also show that the liquid particles are predominantly represented by filaments and films (approximately cylinders and plates) with transverse flow. From this it can be concluded that the tangential forces, or the gas viscosity, exert a considerably smaller effect on the atomization than the pressure forces or the gas density.

The gas viscosity will, however, exert a greater effect on the forward motion of the small drops which, owing to the smaller dimensions and relative velocities, takes place at correspondingly smaller Reynolds numbers. This would exert a certain effect on the propagation velocity and shape of the atomization jet but will not greatly affect the size of the formed drops.

For a quantitative check of the effect of the gas viscosity, or the ratio M, atomization tests were carried out with methanol (ρ = 80.6 kg s^2/m^4, μ = 0.643×10^{-4} kg s/m^2 and σ = 23.3×10^{-4} kg/m) for otherwise equal test conditions, but in gases of different viscosity, namely in acetylene with μ_g = 1.04×10^{-6} and M = 1.62×10^{-2}, in air with μ_g = 1.83×10^{-6} and M = 2.85×10^{-2} and in neon with μ_g = 3.17×10^{-6} kg s/m^2 and M = 4.93×10^{-2}.

Figure 12 shows the size distribution for Re = 29,300 and figure 13 for Re = 35,500. As is seen from these figures, the points of the three tests deviate little from a mean distribution curve.

Figure 14 shows the dependence of the mean drop diameter D_m on the criterion M of the atomizations for Re = 29,300 and Re = 35,500. Since the test points differ little in their values the numerical values associated with the points are indicated for greater clarity. It can be seen that with increasing M, or increasing gas viscosity, the mean drop diameter decreases, a result that is to be ascribed to the increase of the friction forces of the gas. It is worthy of note that at the higher Reynolds number the change of the mean drop diameter is smaller: for an approximately three-fold increase of M D_m decreases at Re = 29,300 by 8.6 percent and at Re = 35,500 only by 5 percent. According to the preceding theoretical consideration an even smaller effect of M is to be expected with further increase in the Reynolds number.

In order to be able correctly to estimate the effect of M there was also investigated the effect of the gas density, or of the ratio $N = \rho_g/\rho$, by increasing only the air density through a change of the pressure, with the other conditions remaining the same. Figure 15 shows the drop size distribution of the atomizations for the air densities ρ_g = 0.0257 and N = 0.318×10^{-3}, ρ_g = 0.074 and N = 0.916×10^{-3}, ρ_g = 0.122 and N = 1.51×10^{-3}, ρ_g = 0.240 kg s^2/m^4 and N = 2.98×10^{-3}. It is seen that the effect of the gas density, or of the criterion N, on the drop distribution is rather large. Figure 16 shows the dependence of the mean drop diameter D_m on N; with increasing N, or increasing gas density, the mean drop diameter decreases, a result ascribed to the increase of the pressure forces. For a three-fold increase of N, for example (from 1×10^{-3} to 3×10^{-3}), the mean drop diameter is decreased by about 57 percent. In comparison with this the effect of M is very small.

From the preceding paragraphs we arrive at the conclusion that at larger Reynolds numbers the effect of the gas viscosity, or of the ratio M, is relatively small. The approximate model tests can therefore be carried out without restricting the similarity condition M' = M" (i.e., employing a gas of smaller viscosity). For Reynolds numbers above 35,000, which generally are encountered in practice, an error of the mean drop diameter of less than 5 percent would be committed if, using the same gas,

a model liquid with three times the viscosity were used, which even for $\rho' = \rho''$ and $\sigma' = \sigma''$ makes possible a nine-fold enlargement of the model and a three-fold reduction of the velocities.

VI. RESULTS

From the discussion of the mechanism of the liquid atomization the forces acting during the process were obtained and it was possible to draw conclusions on their order of magnitude. Further, it was possible to set up the equations which express the motions of the liquid and of the gas and the boundary conditions.

By introducing relative measuring units the system of equations describing the process could be reduced to nondimensional form. There were then obtained the required criteria for dynamic similarity and the criterial equation for the drop diameters, which for constant material properties could be greatly simplified.

To check the derived model laws comparison model tests of a hydraulic atomization were carried out. The relatively good agreement of the dimensionless drop size distributions and of the mean drop diameters shows that the criteria appearing in the criterial equation are sufficient for attaining similarity.

Through quantitative theoretical investigation and through tests it was shown that for larger Reynolds numbers the effect of the criterion M, or of the gas viscosity, on the size of the formed drops is relatively small. Approximate model tests without satisfying M for simplified test conditions can therefore be carried out.

The derived model laws permit the modeling of liquid atomizations and provide possibilities for simplifying the experimental investigation of the atomization process, perfecting the atomization apparatus and generalizing the results of measurements.

REFERENCES

1. Lohnstein, T.: Zur Theorie des Abtropfens mit besonderer Rücksicht auf die Bestimmung der Kapillarkonstanten durch Tropfenversuche, Annalen der Phys., 1906, p. 20.

2. Haenlein, A.: Über den Zerfall eines Flüssigkeitsstrahles. Z.A.M.M., 1931.

3. Weber, C.: Zum Zerfall eines Flüssigkeitsstrahles. Z.A.M.M., 1931.

4. Hochschwender, E.: Über das Zerblasen von Wassertropfen im Luftstrom und die Wasserfalltheorie der Gewitter. Dissertation, Heidelberg, 1919.

5. Kirpitschev, M. V.: Theory of Similarity. AN SSSR (Russian), 1953.

6. Eigenson, L. S.: Model Theory, Gosizd. "Sovetskaya Nauka", Moscow (Russian), 1952.

7. Weber, M.: Die Grundlagen der Ähnlichkeitsmechanik und ihre Verwertung bei Modellversuchen unter besonderer Berücksichtigung schiffbautechnischer Anwendung, Jahrbuch der Schiffbautechnischen Gesellschaft, 1918.

8. Ohnesorge, W.: Die Bildung von Tropfen an Düsen und die Auflösung flüssiger Strahlen. Z.A.M.M., 1936.

9. Lindner, K.: Modellversuche an Druckrohrleitungen. Wasserwirtschaft, 1934.

Translated by S. Reiss
National Aeronautics and
Space Administration

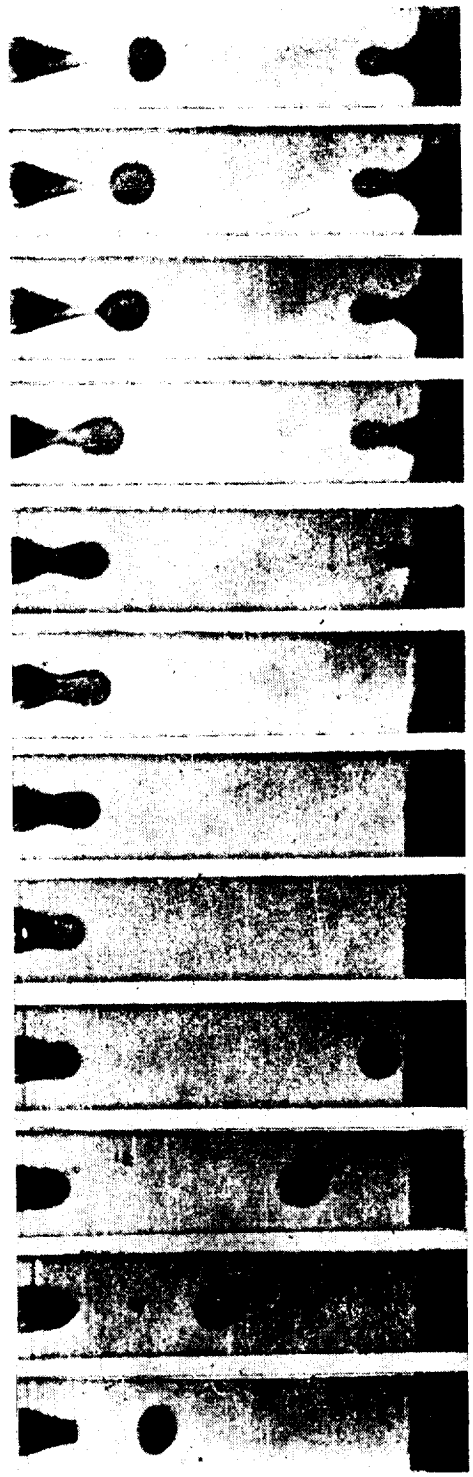

Figure 1. - Dripping under action of gravity.

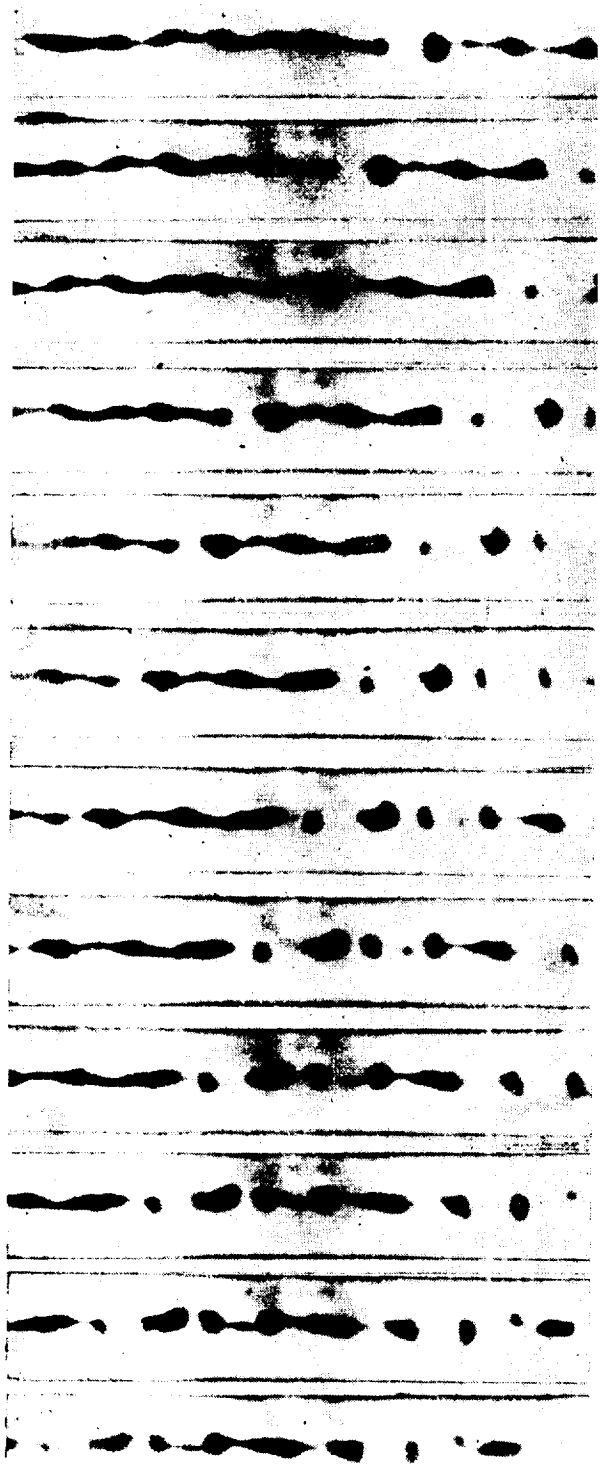

Figure 2. - Drop formation of liquid jet under action of surface tension.

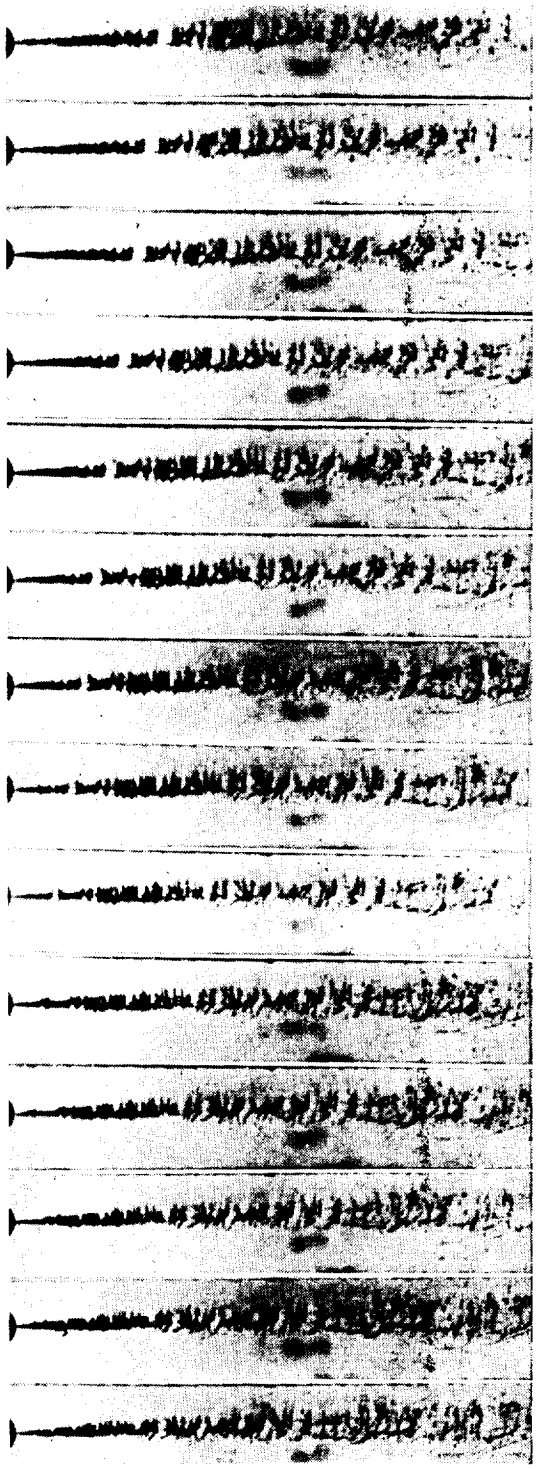

Figure 3. - Turbulent jet disintegration in vacuum.

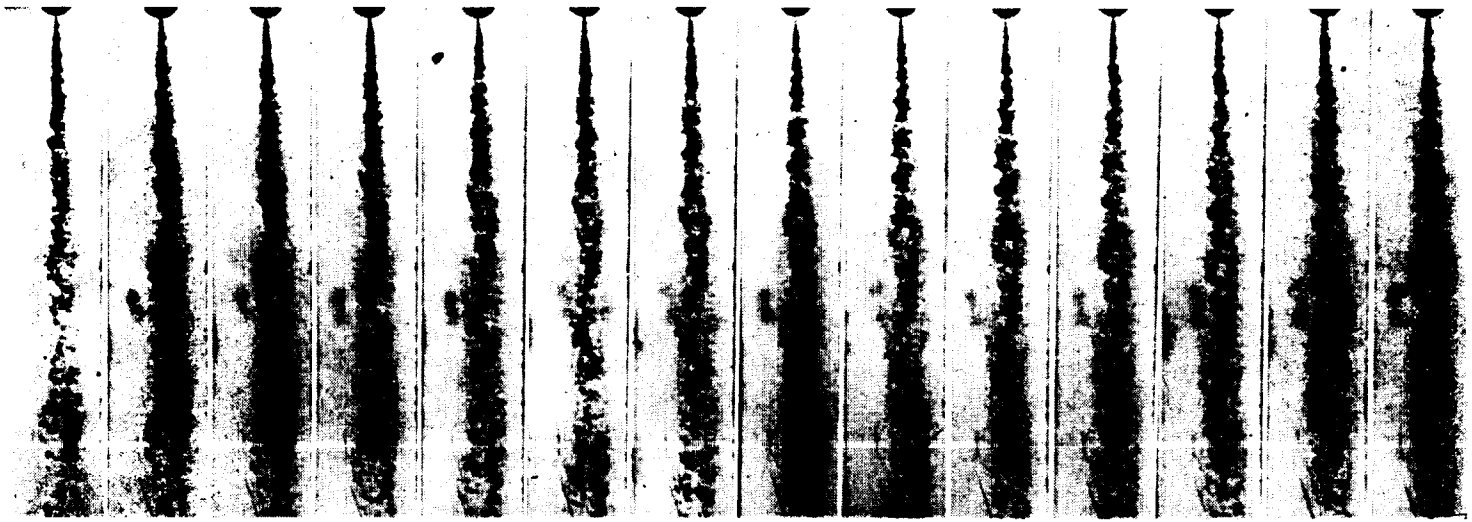

Figure 4. - Jet disintegration in air under atmospheric pressure.

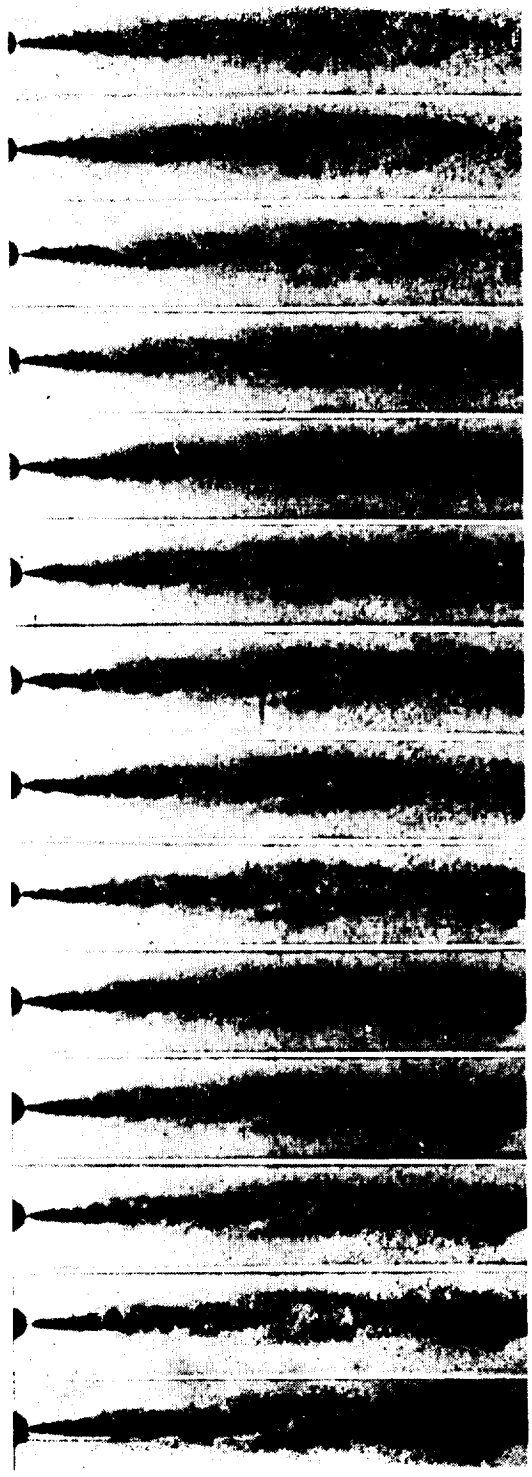

Figure 5. - Jet disintegration in air under excess pressure of 2 atmospheres.

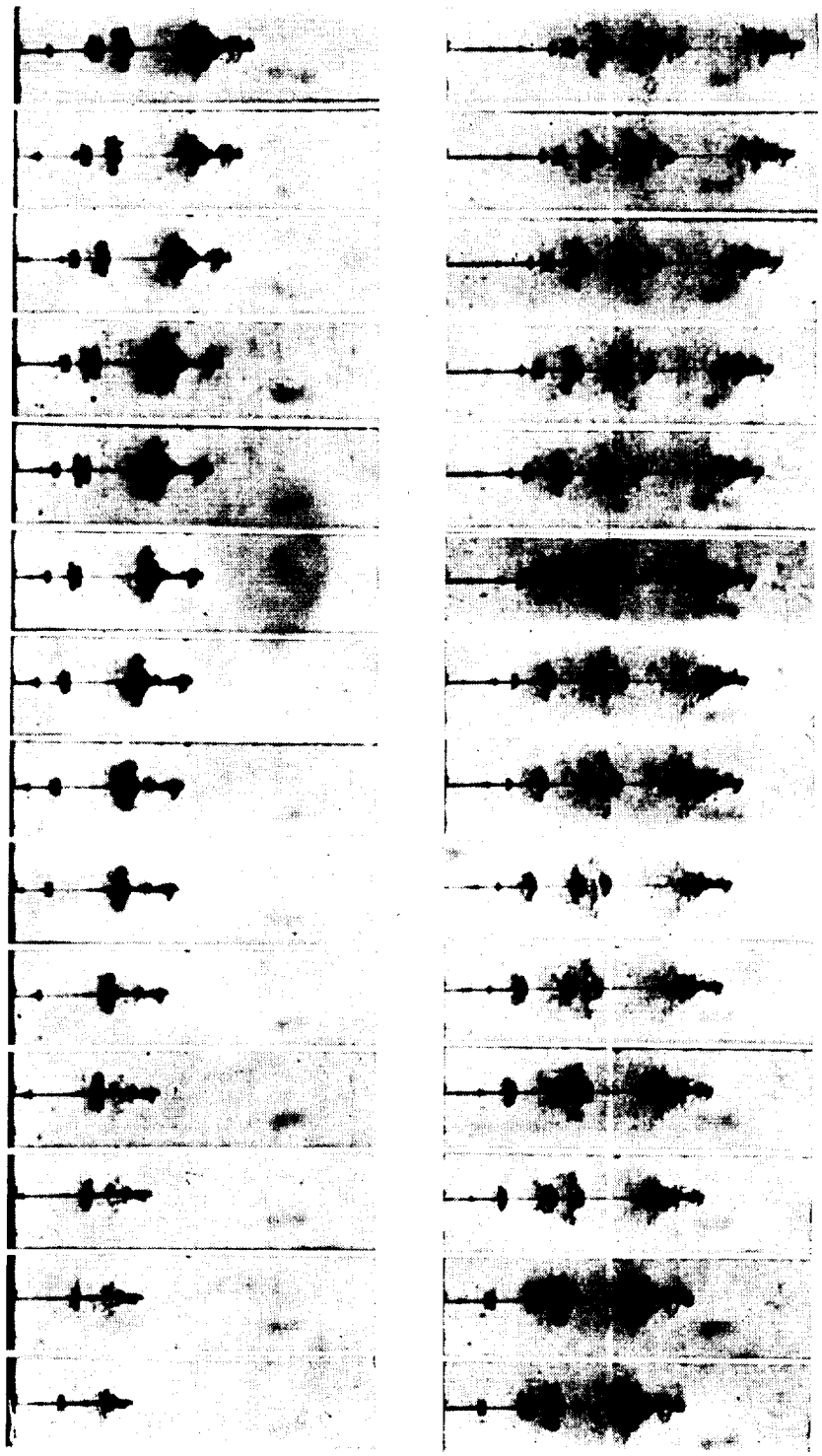

Figure 6. - Blowing apart process under action of gas forces.

E-1095

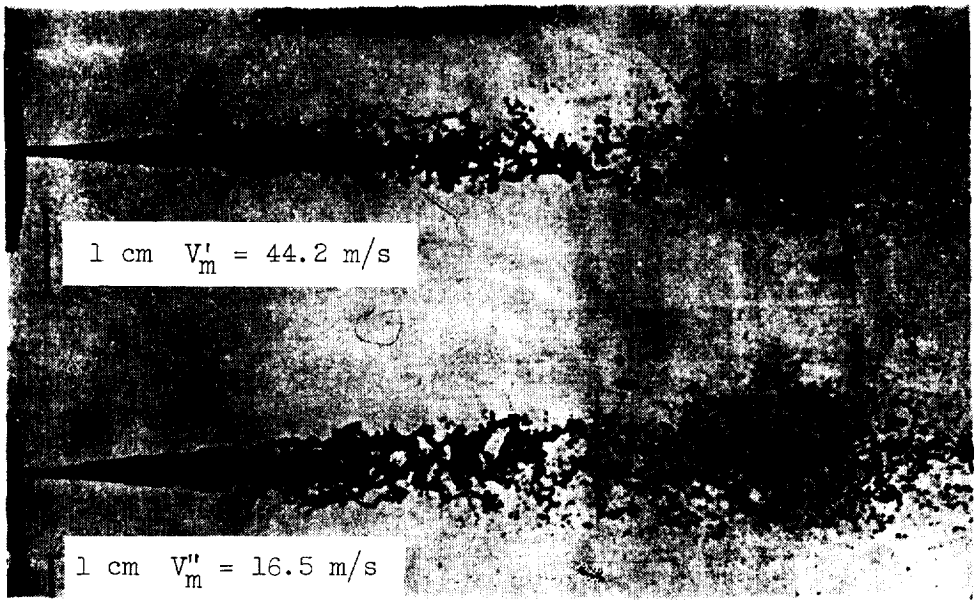

Figure 7. - Similarly setup atomization jets for Re = 41,800, $Z = 0.39 \times 10^{-2}$, $N = 1.2 \times 10^{-3}$, and $M = 1.7 \times 10^{-2}$.

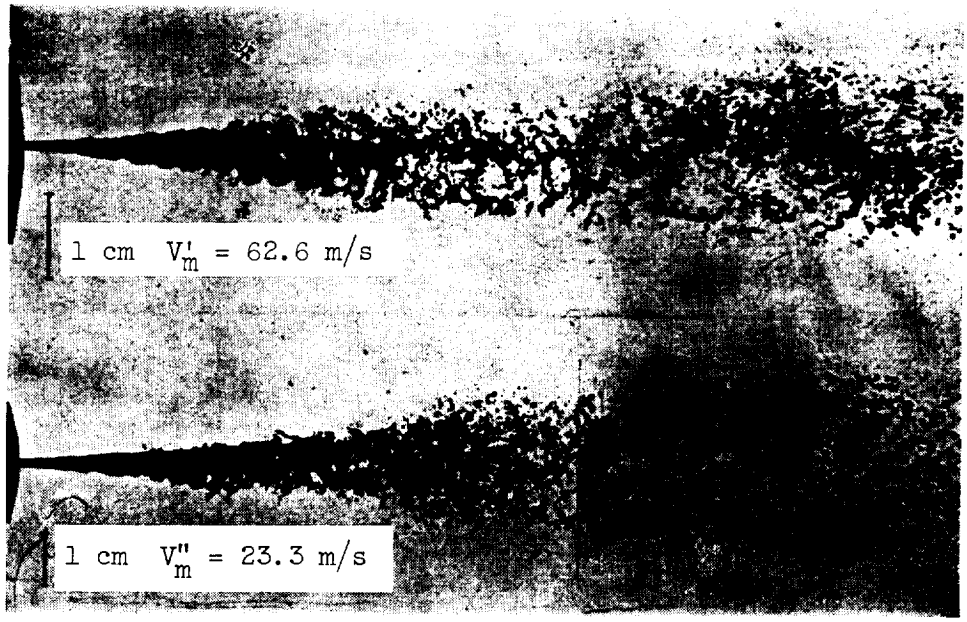

Figure 8. - Similarly setup atomization jets for Re = 59,100, $Z = 0.39 \times 10^{-2}$, $N = 1.2 \times 10^{-3}$, and $M = 1.7 \times 10^{-2}$.

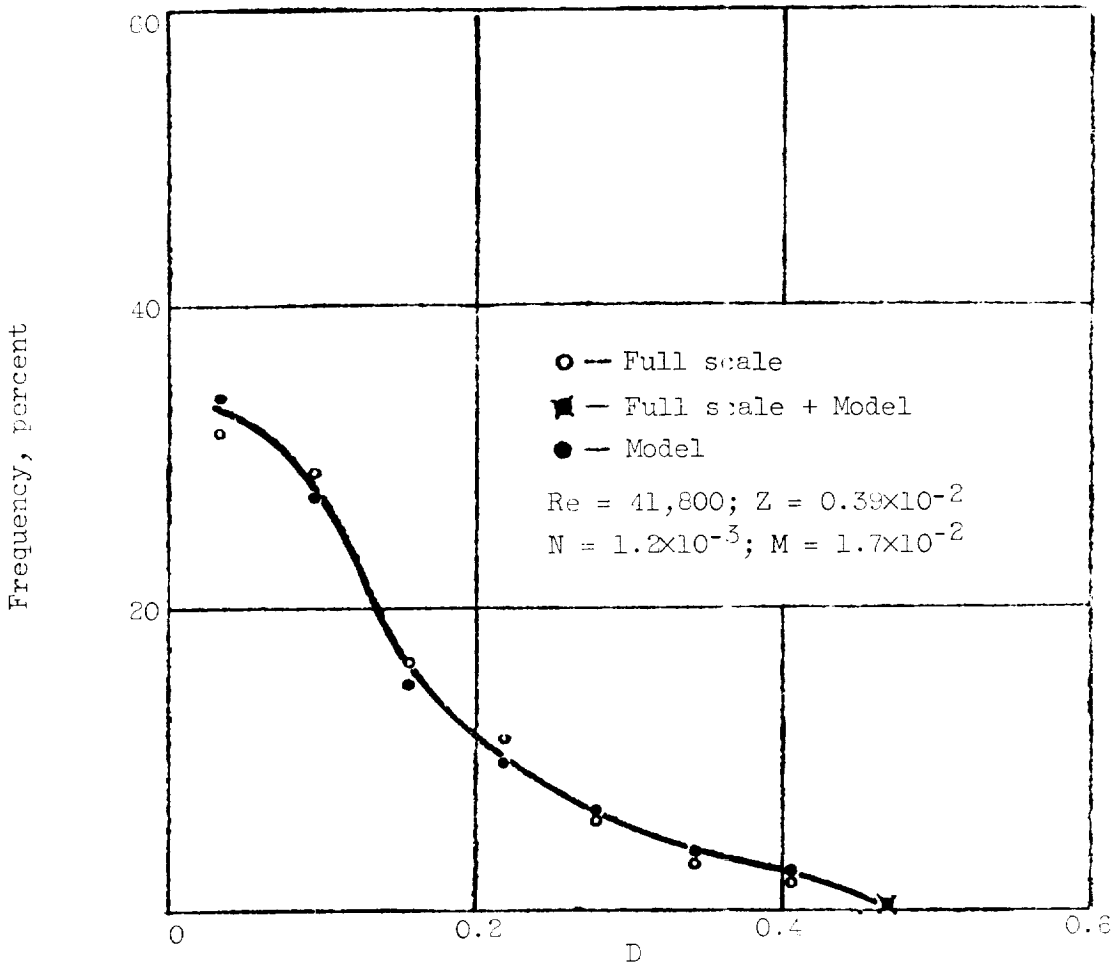

Figure 9. - Drop size distribution of two similarly setup atomizations.

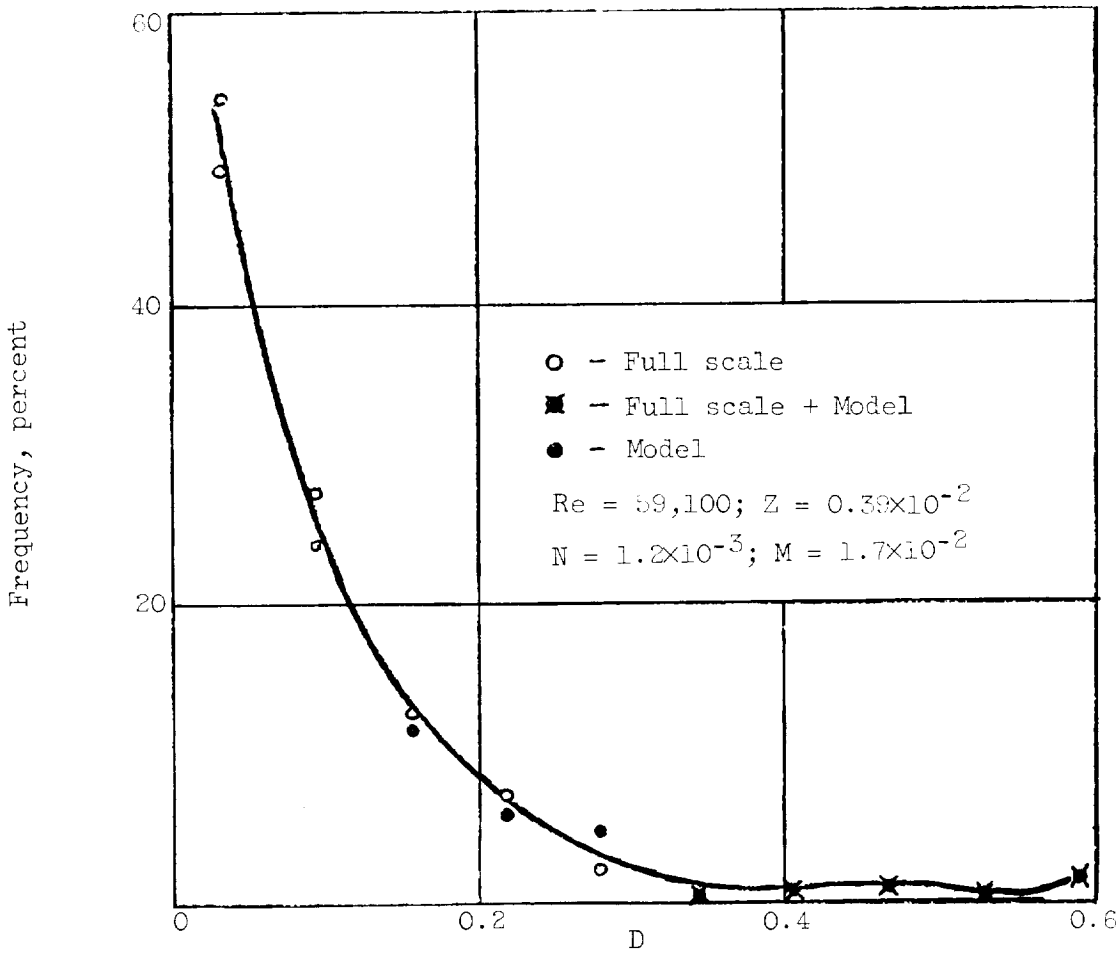

Figure 10. - Drop size distribution of two similarly setup atomizations.

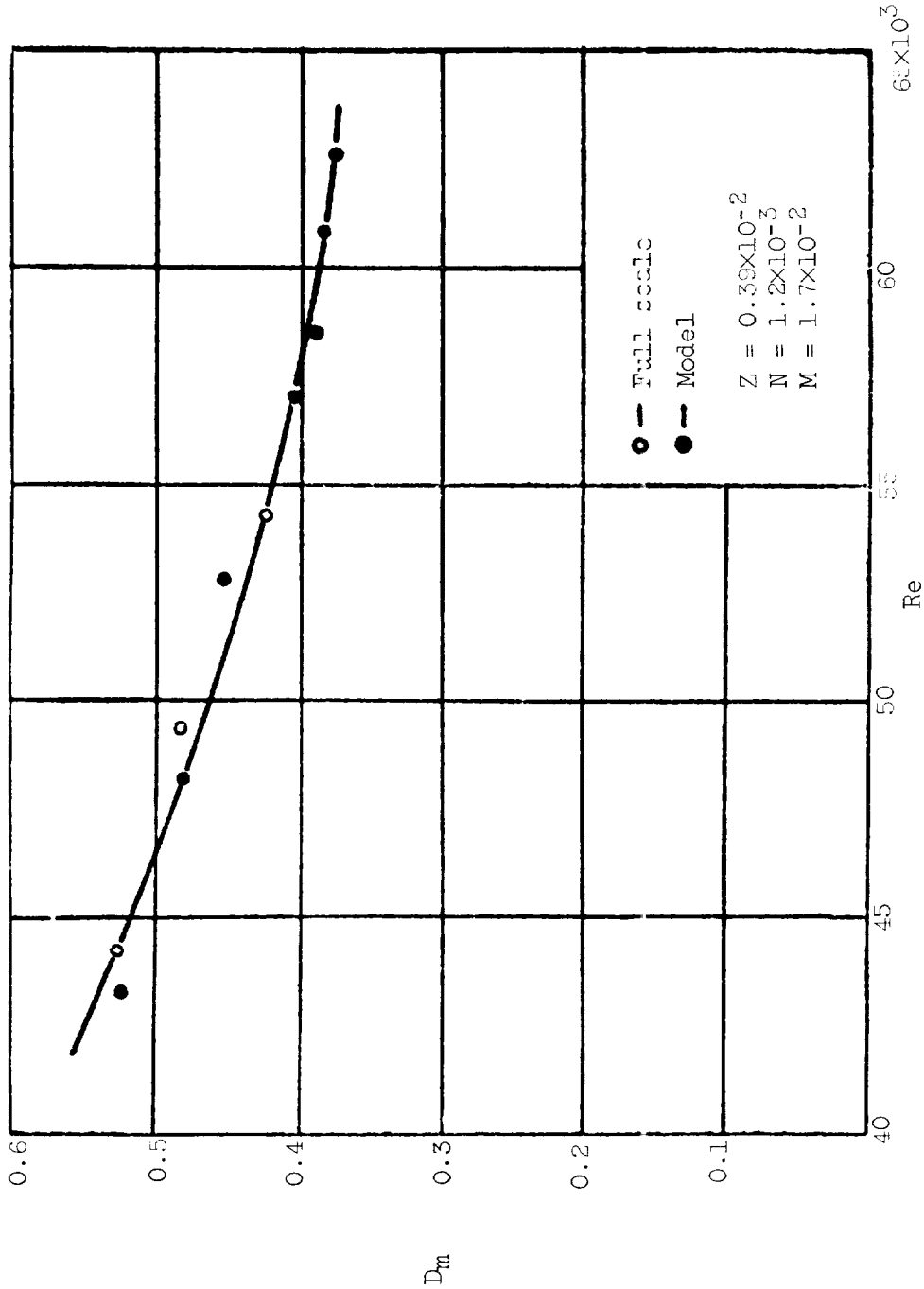

Figure 11. - Mean drop diameter as function of Reynolds number.

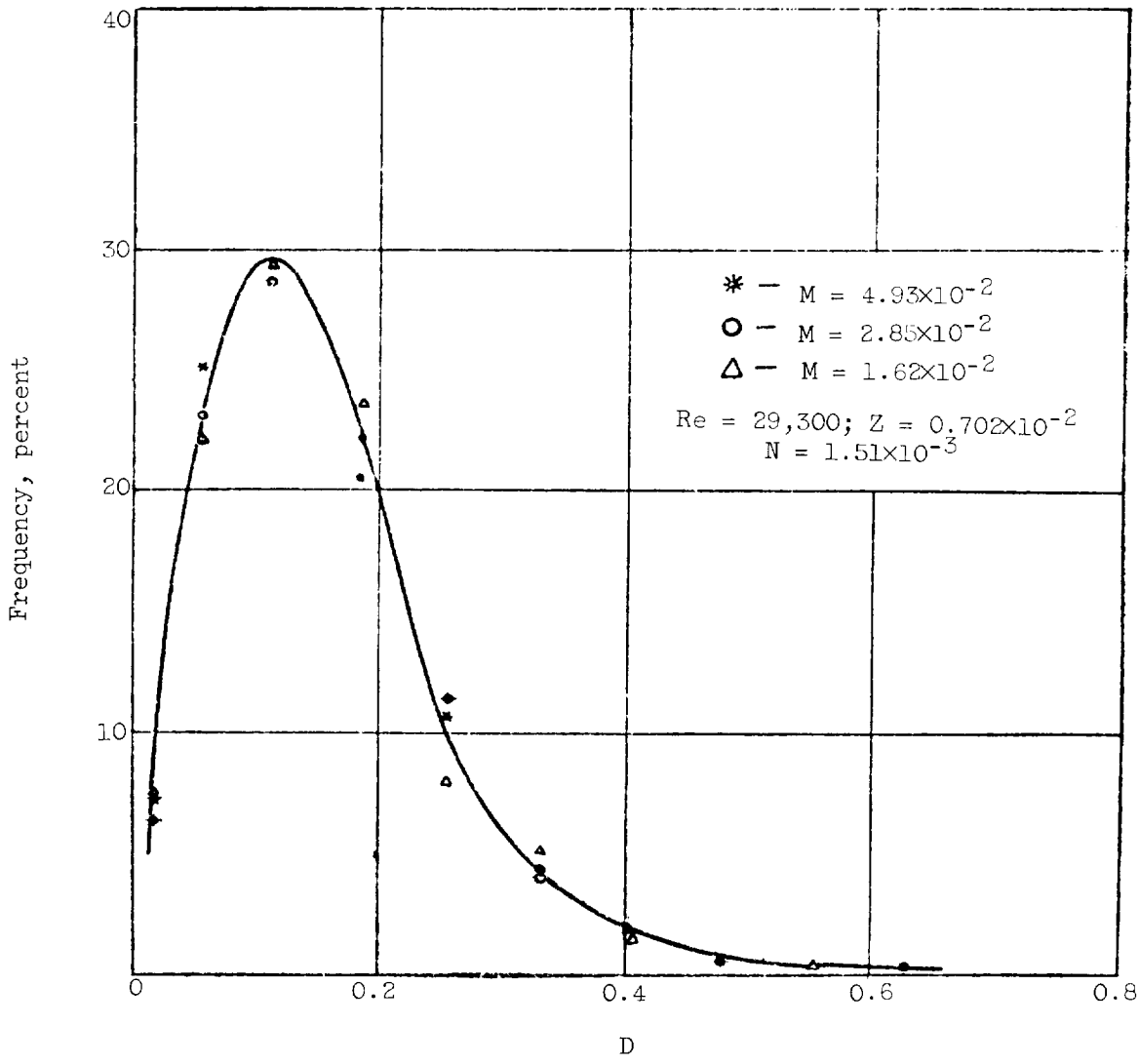

Figure 12. - Drop size distribution for various gas viscosities.

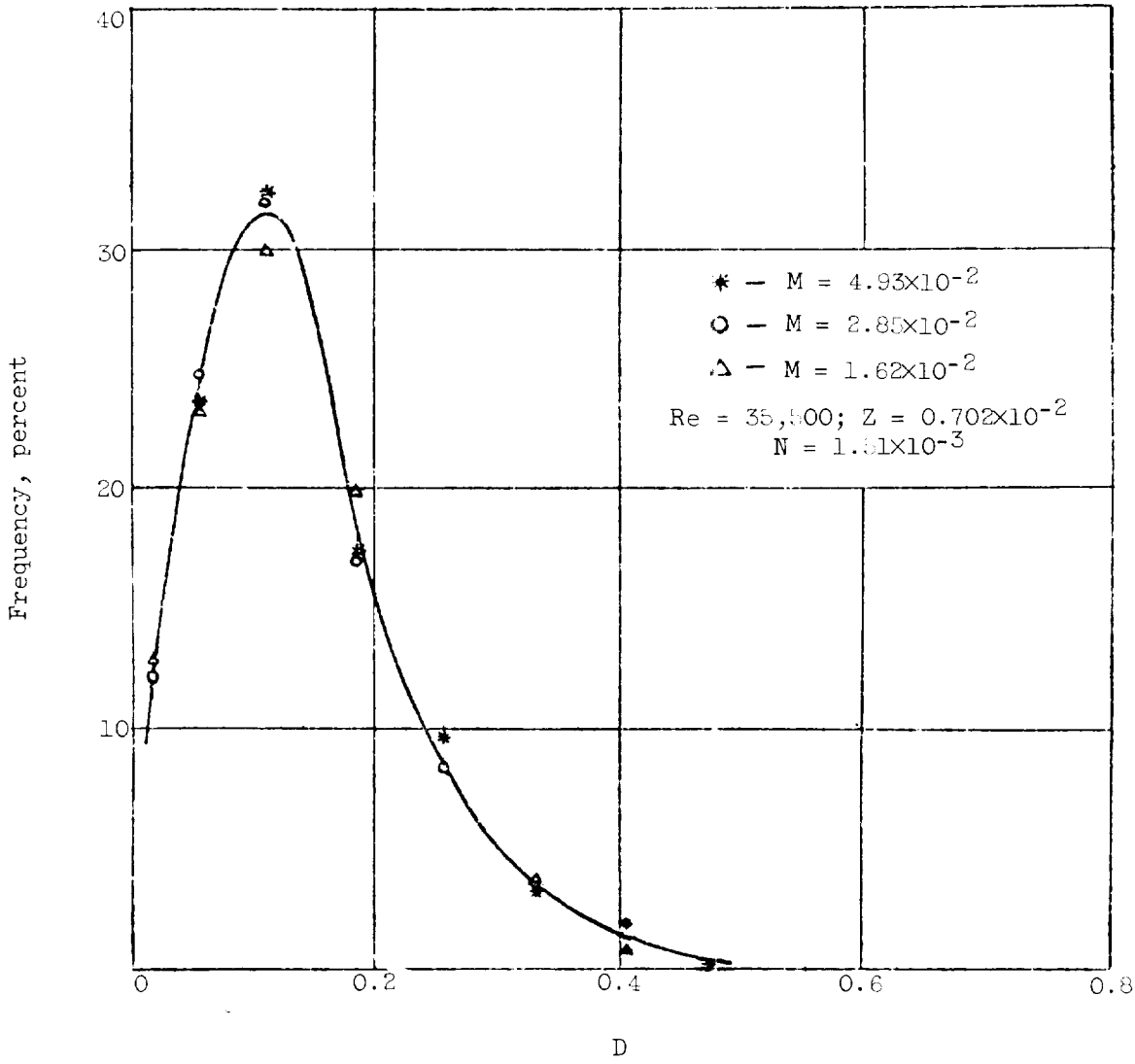

Figure 13. - Drop size distribution for various gas viscosities.

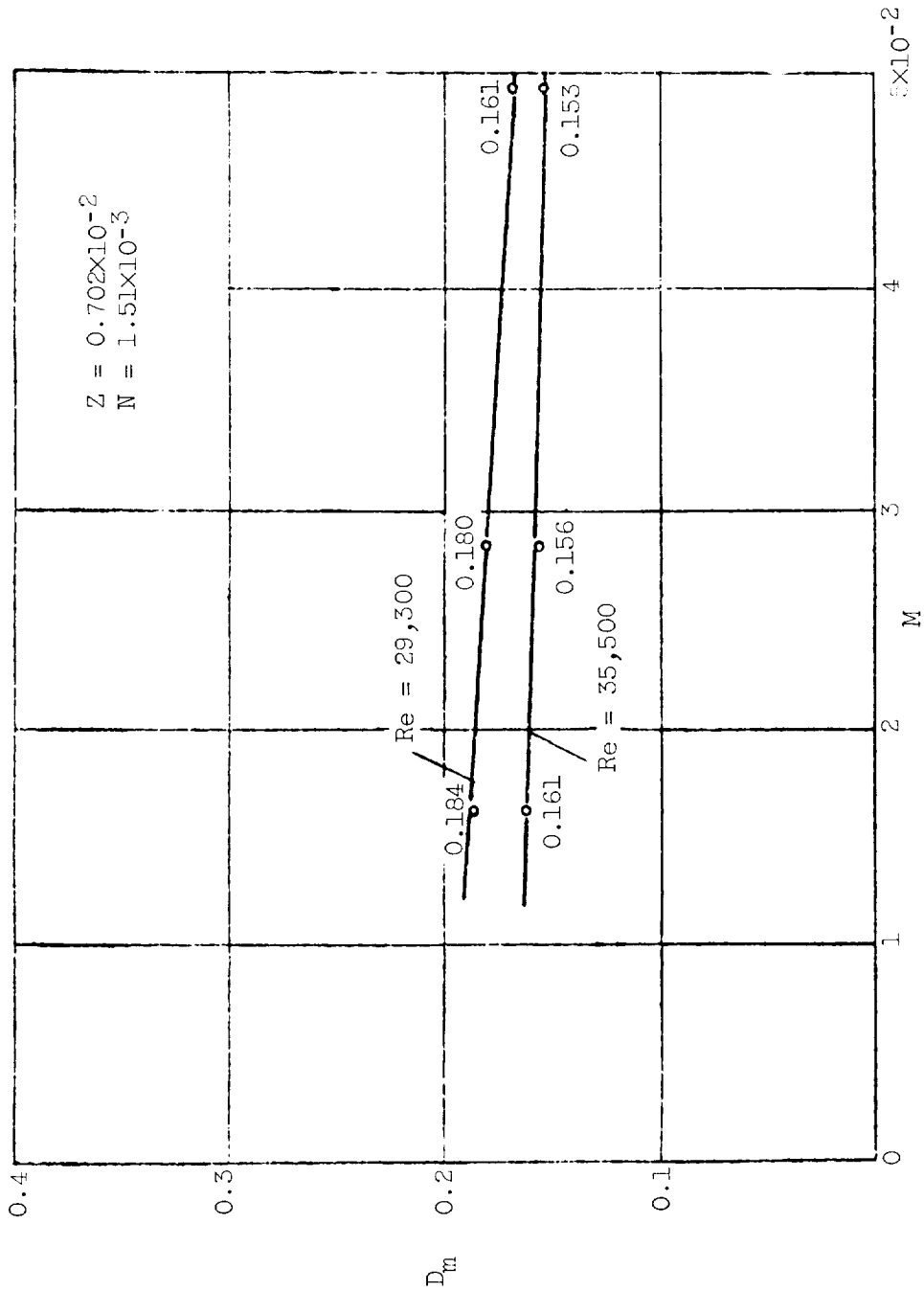

Figure 14. - Mean drop diameter as function of gas viscosity.

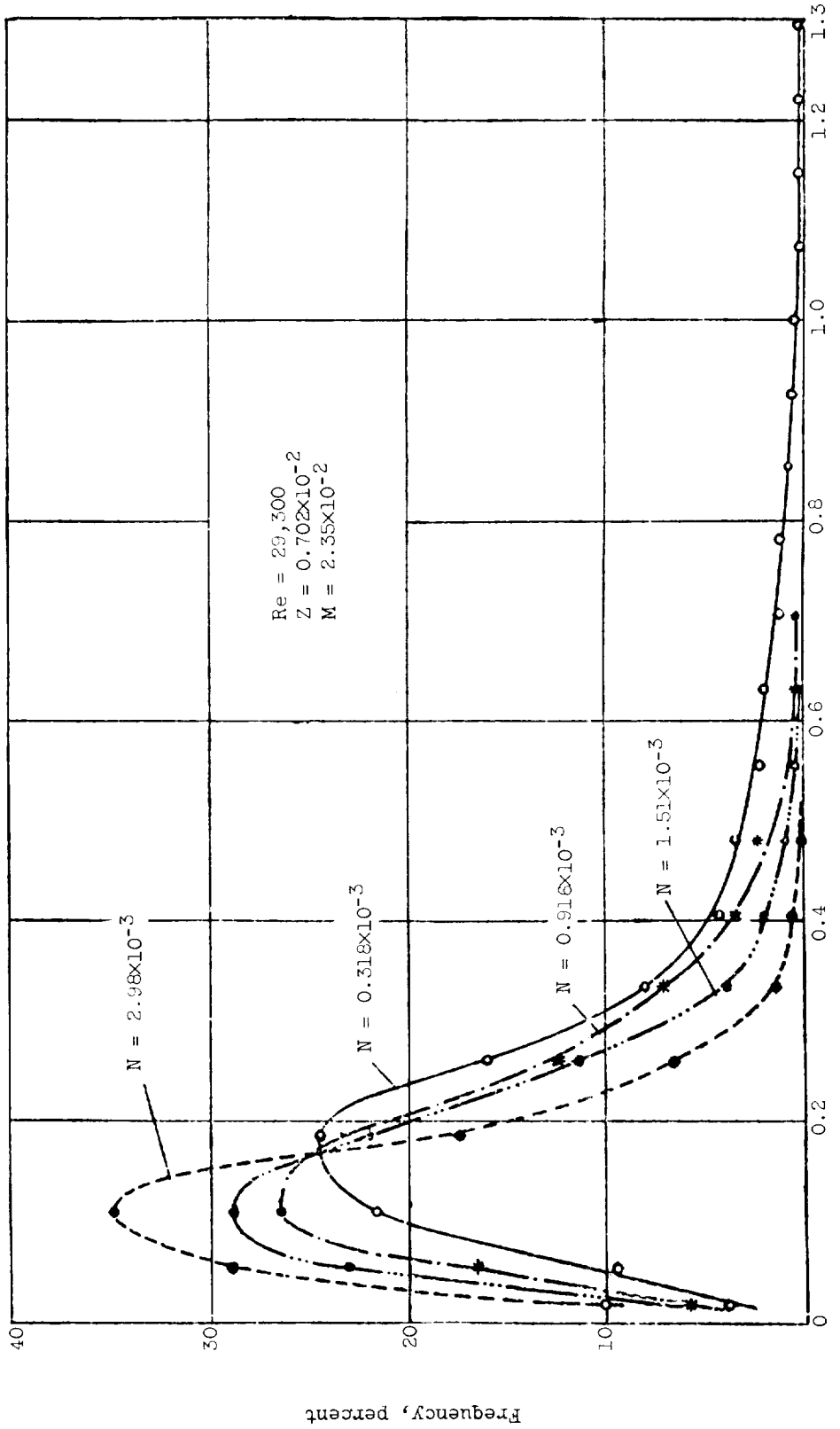

Figure 15. - Drop size distribution for various gas densities.

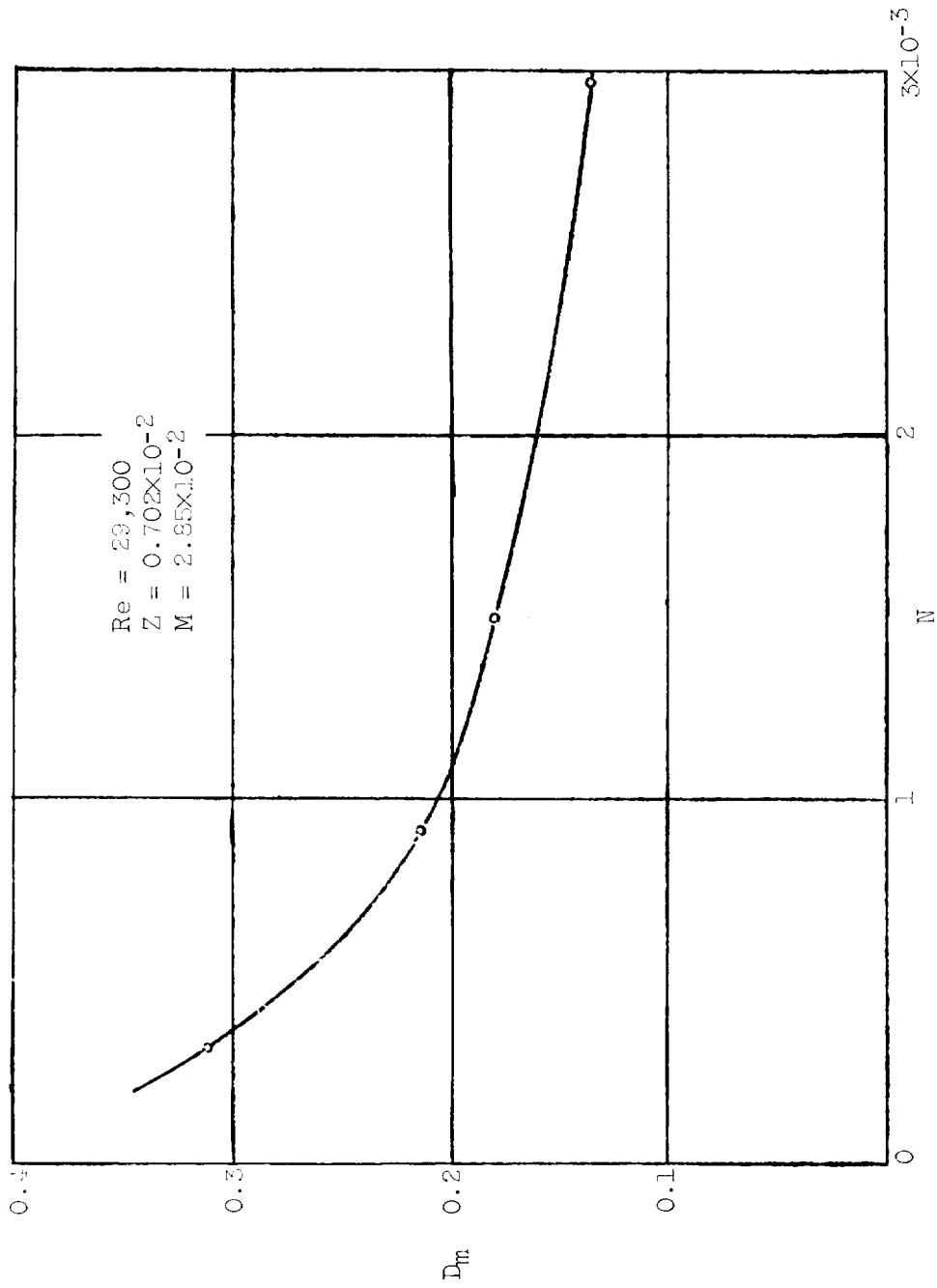

Figure 16. - Mean drop diameter as function of gas density.